

Investigating Polypropylene–Green Coconut Fiber Composites in the Molten and Solid States through Various Techniques

Jean L. Leblanc,¹ Cristina R. G. Furtado,² Marcia C. A. M. Leite² Leila L. Y. Visconte³
Marina H. Ishizaki³

¹*Univ. P. & M. Curie (Paris 6), Polymer Rheology and Processing, France*

²*Univ. Est. Rio de Janeiro, Inst. Química, Rio de Janeiro, Brazil*

³*Univ. Fed. Rio de Janeiro, Inst. Macromol. Prof. I Mano, Rio de Janeiro, Brazil*

Received 19 December 2005; accepted 30 January 2006

DOI 10.1002/app.24239

Published online in Wiley InterScience (www.interscience.wiley.com).

ABSTRACT: A series of polypropylene (PP)–green coconut fiber (GCF) composites were prepared by melt mixing and their properties studied in the molten state using an advanced nonlinear harmonic testing technique, and in the solid state using standard mechanical testing and scanning electron microscopy (SEM). The effect of fiber loading as well as the role of maleated polypropylene as compatibilizing agent was investigated. PP–GCF composites are heterogeneous materials that, in the molten state, are found to exhibit essentially a nonlinear viscoelastic character, in contrast with the pure PP, which has a linear viscoelastic region up to 50–60% strain. Complex modulus increases with GCF content but in such a manner that the observed reinforcement is at best of hydrodynamic origin, without any specific chemical interaction occurring between the polymer matrix

and the fibers. The addition of maleated polypropylene improves the wetting of fibers by the molten polymer but the effect is so small that specific chemical reactions could hardly be considered as occurring. Flexural modulus data confirm the reinforcing effects of the fiber and an improvement is noted when some maleated polypropylene is used, with an optimum level of around 1% (or the PP content). SEM microphotographs clearly show that maleated polypropylene imparts a better wetting of GC fibers by PP, but chemical interactions are unlikely to occur between the polymer and GCF. © 2006 Wiley Periodicals, Inc. *J Appl Polym Sci* 102: 1922–1936, 2006

Key words: fibers; composites; modulus; viscoelastic properties; polypropylene; reinforcement

INTRODUCTION

In Brazil, empty Green Coconuts are available in huge quantities, as coconut water is locally a traditional drink. Between the outer shell of the coconut and the central nut, there is a thick white and fibrous material, which, on drying, yields long yellowish fibers and a brown powdery stuff. When mixing thermoplastic polymers with (dried) green coconut fibers (GCF), interesting composites can be prepared with obvious economical and environmental advantages, in line with present development in the field of so-called “wood–polymer composites.” Polymer–GCF composites are by nature complex materials and, as such, offer challenging scientific and technical problems, namely in terms of viscoelastic properties in the molten state and of mechanical properties in the solid state, with of course the underlying difficulties in understanding the interactions between the fibers and the matrix.

The aims of this report are to present results obtained within the frame of an international collaboration for studying GCF–polymer composites. More precisely, polypropylene (PP) based composites have been prepared on the laboratory floor and their properties studied, in the molten state using an advanced nonlinear harmonic testing technique, and in the solid state using standard mechanical testing and scanning electron microscopy (SEM). Because the work reported involved collaborations between several partners mastering different disciplines, authors’ specialized contributions will be specified when appropriate, in agreement with recommendations by many scientific societies.¹

MATERIALS

Polymer and other compounding ingredients

Polypropylene (PP 1074) was supplied by ExxonMobil Chemical (Houston, TX): specific gravity is 0.9 g/cm³ and MFI (230°C) is 20 g/10 min. Maleated polypropylene (PO 1020), supplied by ExxonMobil Chemical, was used as (expectedly) a coupling agent in PP–GCF compositions; specific gravity is 0.9 g/cm³ and maleic anhydride content is 0.75%. GCF were supplied by Projeto Coco Verde. Rio de Janeiro, Brazil.

Correspondence to: J. L. Leblanc (jean.leblanc@ifoca.com).
Contract grant sponsor: CAPES-COFECUB.

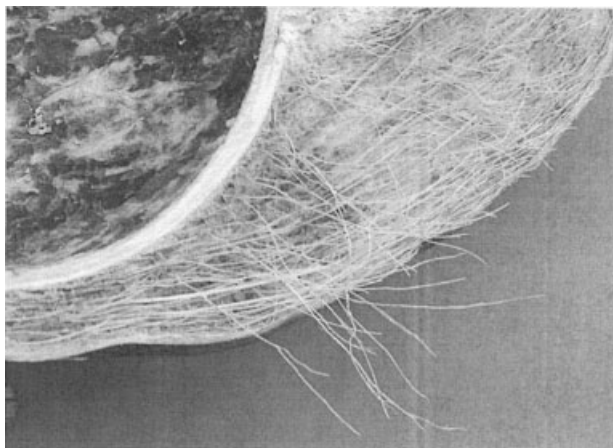


Figure 1 Fibers out of drying green coconut.

Green coconut fibers (GCF)

GCF manufacturing process

GCF are a by-product of empty coconuts waste, available in large quantities in the coastal regions of Brazil, after drinking green coconut water. Each coconut weighs ~700 g, and between the green thin outer shell and the central hard nut that contains the water, there is a 3–4 cm thick white and fibrous material. On drying this intermediate core resumes in long yellowish fibers of up to 10 cm long (Fig. 1). The material used in this study results from a complex process, which involves drying, grinding, and sorting of fibers from green coconut shells.

Analyzing GCF

GCF samples used in this study consisted of a mixture of a fine brown powder with dispersed yellow–orange single fibers of up to 3–4 cm length before grinding (Fig. 2). GCF samples passed through a mesh 40 sieves

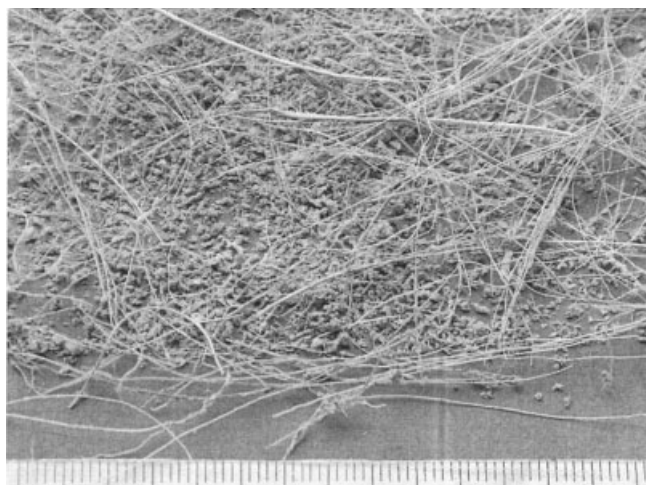


Figure 2 Typical sample of green coconut fibers before grinding and sorting.

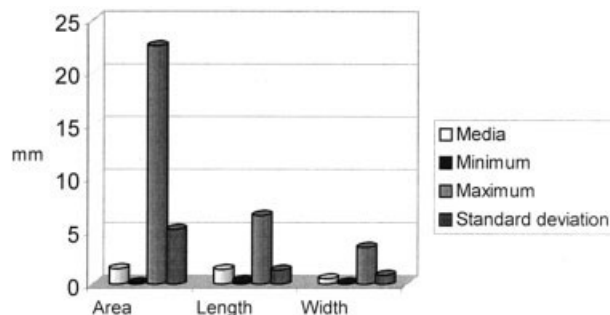


Figure 3 Coconut fibers dimensions after passing through a 40 mesh sieve.

and their specific gravity was 1.20 g/cm³. Before preparing PP–GCF composites, fibers were air-dried for 24 h at 80°C and for at least 1 h at 110°C until stabilization of moisture content reached around 4%.

Typical GCF samples were characterized using an Olympus optical microscopy: model BX50, to determine average dimensions of fibers. Results are given in Figure 3, in terms of average (projected) area, length, and width of coconut fibers. Average (projected) area is 1.48 ± 5.18 mm²; average length, 1.40 ± 1.34 mm; and average width, 0.52 ± 0.86 mm. Measured dimensions are thus largely scattered, quite expectedly for a fibrous material of natural origin. Fibers with length between 1 and 3 cm would be considered ideal for polymer reinforcement, but the average length of the fiber sample used in the present work was found inferior to such ideal values.

PP–GCF composites

The experimental work reported here consisted in evaluating various aspects of PP–GCF composites: (1) effects of preparation (i.e., mixing) conditions, (2) effects of GCF content, and (3) effects of a compatibilizer (at constant GCF loading). Note that, when in use, compatibilizer level was 1, 2, or 3% of PP content. Tables I and II give the formulations of all the samples prepared.

TABLE I
PP-GCF Composites for Studying GCF Level Effects

Sample code	PP ^a (g)	GCF ^b (g)
PP100	100	–
PP090	90	10
PP080	80	20
PP070	70	30

^aPolypropylene PP 1074—supplied by ExxonMobil Chemical, USA; density 0.9 g/cm³, MFI (230°C) 20 g/10 min.

^bGreen coconut fibers, supplied by PROJETO COCO VERDE S.A., Rio de Janeiro, Brazil.

TABLE II
PP-GCF-PO Composites for Studying Compatibilizer Level Effects

Sample code	PP ^a (g)	GCF ^b (g)	PO ^c (g)
PPO_07	70	30	0.7
PPO_14	70	30	1.4
PPO_21	70	30	2.1

^aPolypropylene PP 1074, supplied by ExxonMobil Chemical; density 0.9 g/cm³, MFI (230°C) 20 g/10 min.

^bGreen coconut fibers, supplied by PROJETO COCO VERDE S.A., Rio de Janeiro, Brazil.

^cMaleated polypropylene PO 1020, supplied by ExxonMobil Chemical, USA; maleic anhydride content: 0.75%; density 0.9 g/cm³.

On the laboratory floor, dry blending of ingredients, followed by melt mixing is an easy method to browse preparation conditions. All compositions were consequently melt mixed in a Haake Rheocord 900, fitted with a 85 cm³ mixing chamber with cam rotors, using various conditions, i.e., 170, 180, or 190°C, with cam rotors speed either 20 or 60 rpm. After mixing, samples were compression molded under 7 MPa at 185°C for 2 min, and then cooled for 5 min under the same pressure, before demolding. All samples were kept in plastic bags at room temperature. To have sufficient material for the various experimental works, several

preparation exercises were made with each formulation. Since, for each composition and/or preparation conditions, samples were taken at random for the various experiments of the work program, results of such experiments include de facto (and purposely) the scatter arising from the laboratory preparation technique used.

EXPERIMENTAL RESULTS

Rheological analysis

Fourier transform rheometry: Test protocols, data treatment, and analysis techniques

Like most other complex polymer systems, polymer-GCF composites are expected to exhibit a strong nonlinear viscoelastic character that needs special testing techniques to be studied. Closed cavity torsional rheometers allow for instance, large amplitude harmonic testing to be performed on a variety of stiff (and heterogeneous) materials, which cannot be conveniently tested with standard open gap rheometers. Because direct strain-stress proportionality is lost in the nonlinear domain, appropriate modifications must be brought to commercially available instruments² to capture strain and torque signals, and to treat it with suitable calculation techniques.^{3,4} A closed cavity tor-

RPA-FT; 180°C; 1 Hz; strain = 27.5° (384%)

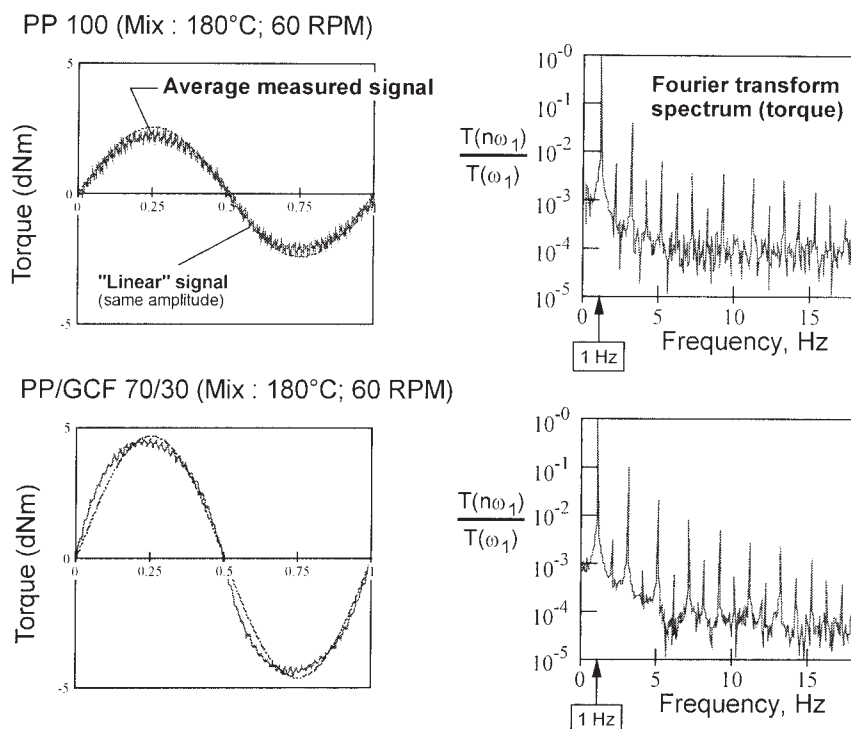


Figure 4 Typical LAOS and Fourier transform experimental results on the unfilled polypropylene and the PP/GCF 70/30 composite.

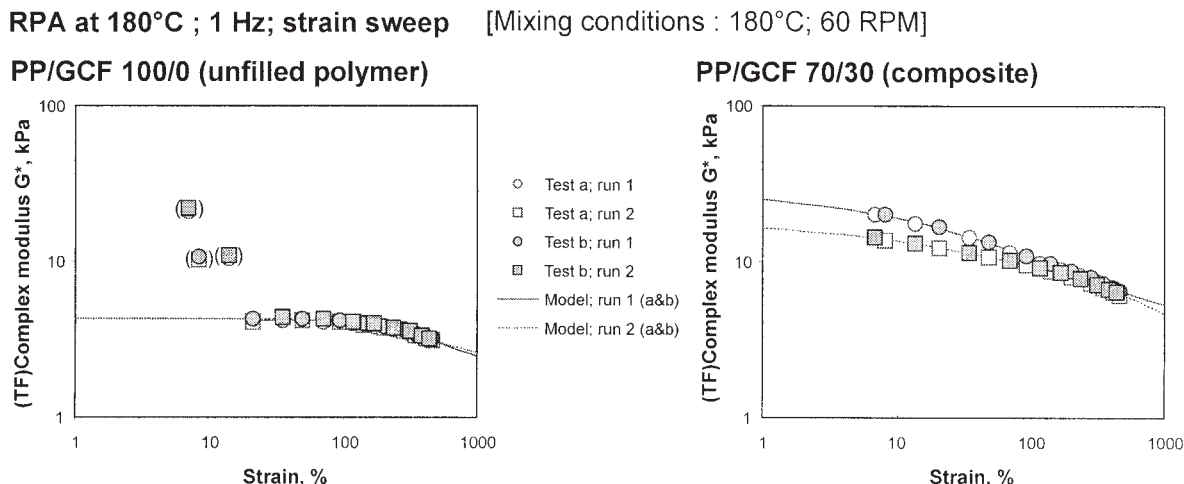


Figure 5 Variation of FT complex modulus with strain amplitude for the unfilled PP and the 30% GCF compound; brackets in the left graph indicate obviously wrong data at low strain.

sional rheometer, such as the so-called “Rubber Process Analyzer” (RPA® 2000, Alpha Technologies), was recently proved to give reliable and reproducible results with PVC–GCF composites, providing the appropriate sample handling technique is used.⁵

With PP–GCF composites, a special sample preparation technique is needed for reproducible results to be obtained, notwithstanding the intrinsic quality of the material. Disks of around 5 cm diameter were first cut out of 1.6 ± 0.1 mm thick molded plaques, then by weighing, their volume was controlled to be within the RPA test cavity volume + around 5% (i.e., 3.15 cm^3). All RPA-FT tests were made at 180°C but it was found that using a starting temperature 20°C higher (when closing the cavity), then cooling down immediately towards the test temperature, gave improved reproducibility with PP–GCF composites, because this technique ensured an excellent filling of the cavity, with a complete closure at

the end of the warming-up period (i.e., 330 s) and thermal homogeneity of the sample.

Figure 4 shows typical results on the unfilled PP sample and the 30% GCF composition, both prepared under the same conditions (mix temperature, 180°C; rotor speed, 60 rpm). Left graphs are average torque signals out of 20 recorded cycles at 1 Hz and 27.5° strain: perfect sinusoids of same amplitude are drawn for comparison. Right graphs are the corresponding FT spectra. As can be seen, torque signals are clearly distorted, which corresponds to a nonlinear character well assessed by the FT spectrum with significant odd harmonics. The PP/GCF composite exhibits, however, a severer distortion of the torque signal, which reflects in higher (relative) odd harmonics, with the third the largest one. One notes incidentally that the torque amplitude is significantly larger for the composite than for the unfilled polymer.

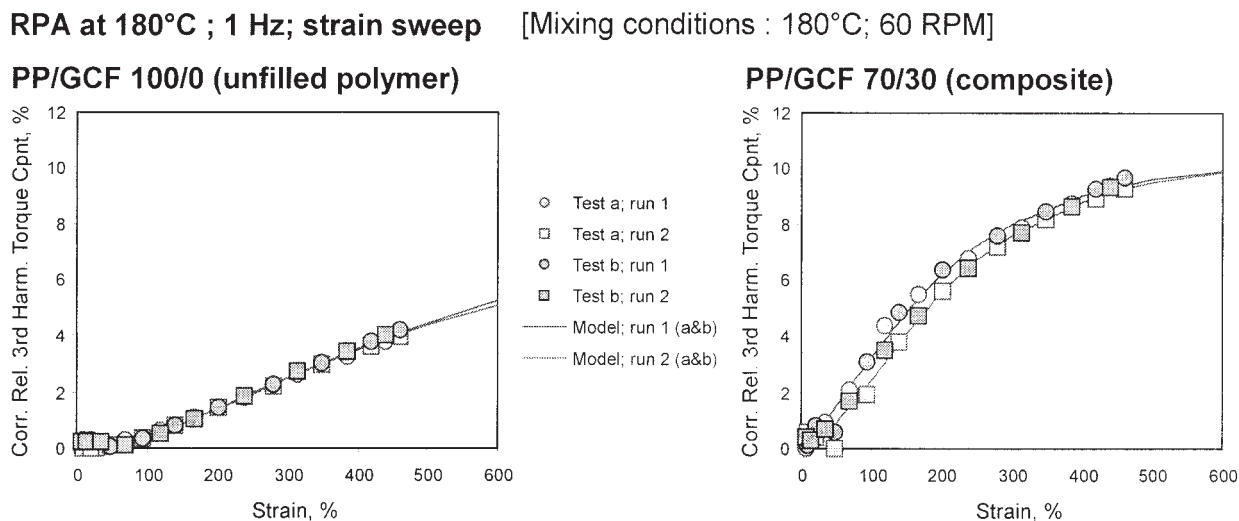


Figure 6 Variation of third harmonic component with strain amplitude for the unfilled PP and the 30% GCF compound.

TABLE III
Fit Parameters for the PP/GCF Composites tested (RPA-FT at 180°C; 1 Hz; Strain Sweep:
Complex Modulus G^* versus Strain)

Mix temp (°C)	Rotor rate (rpm)	Runs (a and b)	G^*_0 (kPa)	G^*_f (kPa)	1/A (%)	B	r^2
<i>PP/GCF = 100/0; modeling G^*_0 versus strain</i>							
190	60	1	4.46	(-0.29)	1238	0.785	0.9836
190	60	2	4.33	0.22	978	0.921	0.9953
180	60	1	4.24	1.74	547	1.535	0.9930
180	60	2	4.26	2.35	387	1.898	0.9803
180	20	1	4.33	1.25	667	1.433	0.9971
180	20	2	4.26	2.57	360	2.092	0.9953
170	60	1	4.57	2.07	470	1.634	0.9909
170	60	2	4.60	1.54	574	1.468	0.9868
170	20	1	4.83	2.22	454	1.420	0.8195
170	20	2	4.91	2.05	476	1.316	0.8348
<i>PP/GCF = 90/10; modeling G^*_0 versus strain</i>							
190	60	1	8.20	0.21	293	0.464	0.9977
190	60	2	5.71	0.50	716	0.988	0.9978
180	60	1	8.26	(-0.16)	448	0.553	0.9973
180	60	2	5.92	1.88	476	1.328	0.9962
180	20	1	9.03	0.73	248	0.584	0.9969
180	20	2	6.31	0.30	716	1.081	0.9980
170	60	1	7.58	(-0.85)	722	0.542	0.9974
170	60	2	5.71	0.98	625	1.227	0.9969
170	20	1	8.00	0.35	404	0.596	0.9980
170	20	2	6.18	(-1.79)	1281	0.889	0.9970
<i>PP/GCF = 80/20; modeling G^*_0 versus strain</i>							
190	60	1	16.00	1.53	51	0.530	0.9981
190	60	2	9.70	(-2.06)	857	0.549	0.9990
180	60	1	19.08	0.44	40	0.425	0.9916
180	60	2	9.80	0.90	443	0.701	0.9945
180	20	1	17.31	1.47	56	0.524	0.9994
180	20	2	9.51	1.54	390	0.879	0.9963
170	60	1	14.57	0.98	83	0.530	0.9994
170	60	2	8.88	(-2.60)	1071	0.653	0.9994
170	20	1	16.63	1.08	56	0.501	0.9938
170	20	2	9.06	(-0.48)	656	0.706	0.9909
<i>PP/GCF = 70/30; modeling G^*_0 versus strain</i>							
190	60	1	25.19	3.36	28	0.667	0.9960
190	60	2	22.13	(-9.71)	399	0.248	0.9978
180	60	1	27.90	2.74	27	0.602	0.9981
180	60	2	20.94	(-11.11)	881	0.269	0.9991
180	20	1	71.52	(-0.15)	2	0.388	0.9965
180	20	2	23.38	1.50	49	0.476	0.9901
170	60	1	41.01	0.63	6	0.411	0.9985
170	60	2	19.25	(-15.34)	2743	0.280	0.9993
170	20	1	44.65	1.47	14	0.501	0.9996
170	20	2	39.87	(-14.12)	54	0.189	0.9993

Proprietary data handling programs, written in MathCad® (MathSoft), are used to perform Fourier transform calculations and other data treatments. Out of Fourier Transform treatment of torque signal, essentially two types of information are extracted: first, the main torque component, i.e., the peak in the FT spectrum that corresponds to the applied frequency [hereafter noted $T(\omega)$], second, the harmonics, with the third (i.e., the peak at $3 \times$ the applied frequency) being the most intense one. FT treatment of the strain signal

provides information about the quality of the applied deformation and allows correcting data for technical limits of the instrument, as explained in details elsewhere.⁶

When dividing the main torque component by the applied strain, i.e., $T(\omega)\gamma$, one gets a quantity that has obviously the meaning of a modulus and, for a material exhibiting linear viscoelasticity within the considered strain amplitude range (not the case for the PPGCF composites), one gets the most familiar picture

TABLE IV
Fit Parameters for the PP/GCF Composites (RPA-FT at 180°C; 1 Hz; Strain Sweep:
Relative Third Harmonic Component $cT(3/1)$ versus Strain)

Mix temp (°C)	Rotor rate (rpm)	Runs (a and b)	$T(3/1)_{\max}$ (%)	C	D	Slope (200%)	r^2
<i>PP/GCF = 100/0; modeling $cT(3/1)$ versus strain</i>							
190	60	1	12.30	0.00139	1.580	0.0090	0.9992
190	60	2	17.96	0.00084	1.366	0.0088	0.9965
180	60	1	8.62	0.00247	1.917	0.0105	0.9977
180	60	2	7.00	0.00328	2.189	0.0109	0.9985
180	20	1	8.29	0.00277	2.235	0.0103	0.9996
180	20	2	8.93	0.00248	2.089	0.0101	0.9993
170	60	1	9.21	0.00235	1.899	0.0106	0.9990
170	60	2	7.45	0.00313	2.189	0.0110	0.9991
170	20	1	7.93	0.00320	2.241	0.0118	0.9903
170	20	2	5.95	0.00449	2.536	0.0124	0.9920
<i>PP/GCF = 90/10; modeling $cT(3/1)$ versus strain</i>							
190	60	1	6.96	0.00393	2.097	0.0134	0.9987
190	60	2	7.33	0.00359	2.096	0.0129	0.9995
180	60	1	6.93	0.00439	2.139	0.0147	0.9984
180	60	2	7.82	0.00352	1.937	0.0139	0.9992
180	20	1	10.69	0.00200	1.299	0.0134	0.9981
180	20	2	8.11	0.00370	2.109	0.0147	0.9990
170	60	1	9.03	0.00292	1.920	0.0133	0.9818
170	60	2	10.31	0.00231	1.702	0.0127	0.9971
170	20	1	13.87	0.00128	1.227	0.0120	0.9914
170	20	2	6.83	0.00466	2.613	0.0146	0.9985
<i>PP/GCF = 80/20; modeling $cT(3/1)$ versus strain</i>							
190	60	1	9.63	0.00305	1.164	0.0163	0.9969
190	60	2	10.88	0.00262	1.300	0.0168	0.9992
180	60	1	8.30	0.00560	1.915	0.0202	0.9972
180	60	2	8.89	0.00549	2.293	0.0221	0.9981
180	20	1	8.90	0.00473	1.684	0.0197	0.9970
180	20	2	8.44	0.00576	2.306	0.0216	0.9966
170	60	1	9.19	0.00397	1.666	0.0184	0.9909
170	60	2	8.16	0.00552	2.542	0.0204	0.9961
170	20	1	7.98	0.00566	1.994	0.0197	0.9968
170	20	2	8.03	0.00556	2.254	0.0201	0.9973
<i>PP/GCF = 70/30; modeling $cT(3/1)$ versus strain</i>							
190	60	1	10.47	0.00513	1.287	0.0218	0.9974
190	60	2	10.96	0.00452	1.421	0.0229	0.9979
180	60	1	10.28	0.00615	1.469	0.0231	0.9969
180	60	2	10.27	0.00639	1.899	0.0259	0.9967
180	20	1	11.42	0.00651	1.023	0.0205	0.9913
180	20	2	11.05	0.00807	1.994	0.0284	0.9962
170	60	1	10.89	0.00424	1.170	0.0210	0.9944
170	60	2	10.57	0.00512	1.706	0.0242	0.9869
170	20	1	10.79	0.00792	1.557	0.0240	0.9980
170	20	2	10.69	0.00821	2.384	0.0301	0.9950

of a plateau region at low strain, then a typical strain dependence. Fourier Transform yields the main torque component in arbitrary units, but with respect to the data acquisition conditions used for Fourier transform calculation, the following equality holds:

$$G^*(\text{kPa}) = 12.335 \times \frac{T(\omega)}{\gamma} \text{ [with } T(\omega) \text{ in arbitrary unit and } \gamma \text{ in \%].}$$

How G^* varies with the applied strain thus offers a direct insight into the nonlinear viscoelastic properties of tested materials. Variations of the

third relative harmonic component, i.e., $T(3\omega)/T(\omega)$ or $T(3/1)$, with the applied strain give another view of the nonviscoelastic character.

RPA-FT results on PP-GCF composites in the molten state

Effects of preparation conditions. Figure 5 shows the FT complex modulus curve as obtained when applying the strain sweep test protocol described above on the

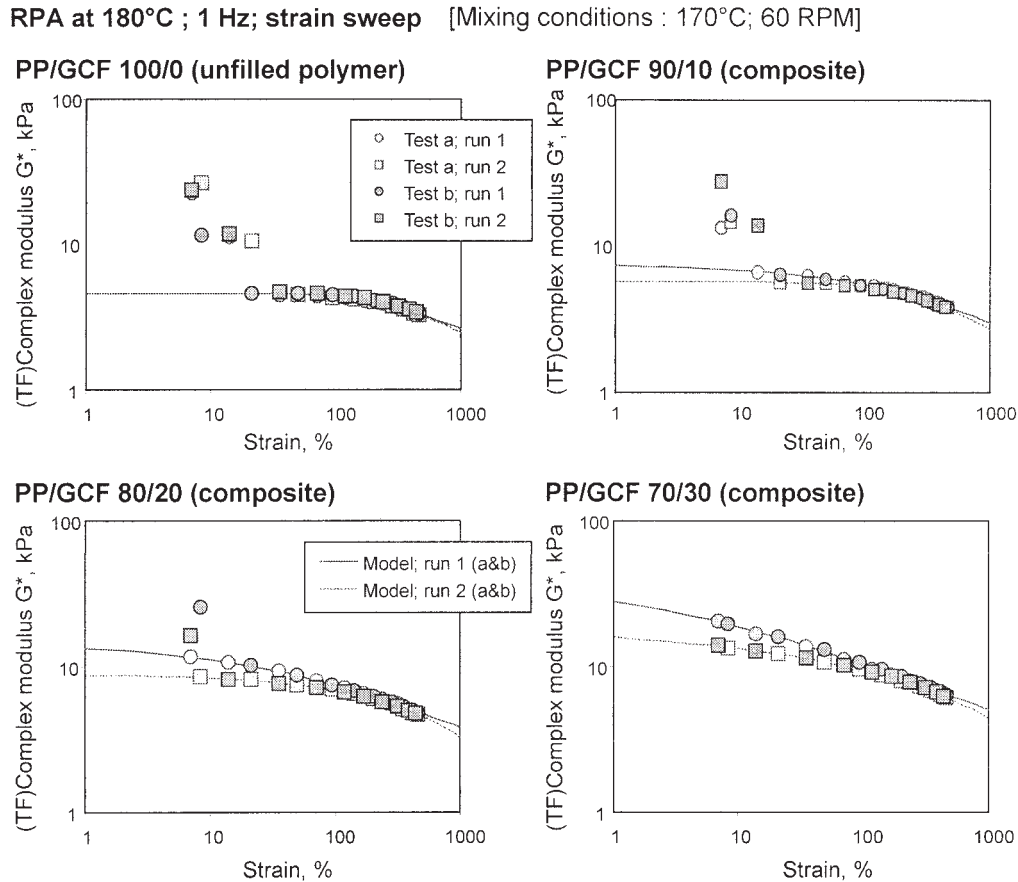


Figure 7 Complex modulus versus strain amplitude for PP/GCF compounds; curves have been drawn using fit parameters given in Table III.

unfilled PP and the 70/30 PP/GCF compound, both prepared under identical mixing conditions. Reproducibility is achieved since results from tests a and b superimpose well. The unfilled PP (left graph) shows no strain history effect and, providing a few obviously wrong results at low strain are discarded, the G^* curve exhibits the expected plateau at low strain then a strain thinning effect above 50–60% strain. Such a behavior is adequately modeled with the following equation:

$$G^*(\gamma) = G_f^* + \left[\frac{G_0^* - G_f^*}{1 + (\Delta\gamma)^B} \right] \quad (1)$$

where G_0^* is the modulus in the linear region; G_f^* the modulus for an infinite strain; A , the reverse of a critical strain (which corresponds to $\frac{G_0^* + G_f^*}{2}$), and B a parameter describing the strain sensitivity of the material. Results with the 30% GCF composite (right graphs) show no linear region within the experimental strain window considered and a clear difference between data gathered during runs 1 and 2. Such data can also be modeled with eq. (1) and the difference

between runs is clearly reflected in the fit curves. Contrary to the unfilled material, PP/GCF composites are thus sensitive to strain history. It must be underlined that both G_0^* and G_f^* are extrapolated features, and therefore of limited meaning, if any, when their numerical value is too far from measured data, which is obviously the case for G_f^* . However, with respect to the curvature of G_0^* curves, G_a^* data for the filled material would therefore be considered with confidence.

Figure 6 displays $T(3/1)$ versus γ curves for the same materials. Data are reproducible (compare tests a and b), and minor differences between runs 1 and 2 appear only for the GCF-filled sample. As previously reported,^{3,5} the variation of the relative third torque harmonic component with the strain amplitude is such that an S-shape curve is generally observed, from zero at low strain up to a maximum at high strain. Even if the maximum $T(3/1)$ is not reached during the experiments, data obtained with the composite (right graph) support the occurrence of a plateau $T(3/1)_{\max}$ outside the experimental strain window. A model, which explicitly considers a maximum $T(3/1)$, can consequently be used to fit $T(3/1)$ versus γ curves. i.e.

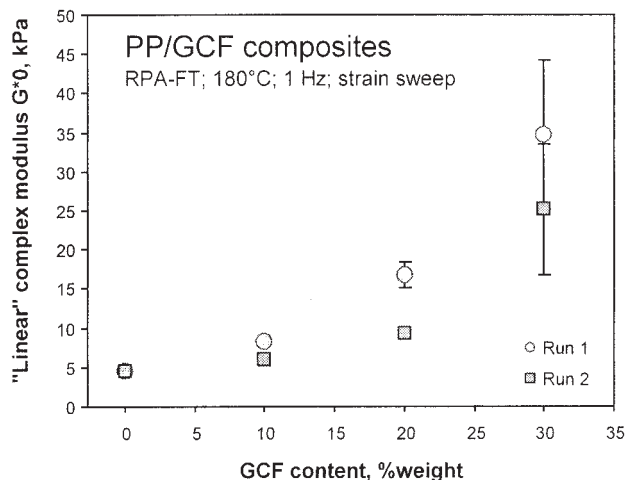


Figure 8 Effect of filler loading on (extrapolated) linear dynamic modulus of PP–GCF composites, irrespective of preparation conditions.

$$T(3/1) = T(3/1)_{\max} \times [1 - \exp(-C\gamma)]^D \quad (2)$$

where γ is the deformation (%), C and D are fit parameters. With respect to the nonlinear viscoelastic behavior, the most significant information is provided by parameters C and D , which “quantify” the strain sensitivity of materials. The first derivative of eq. (2) allows calculating the slope of $T(3/1)$ versus γ curves at any strain, an easier manner to quantify strain effect than simultaneously considering C and D .

Using eqs. (1) and (2) to model G^* versus γ and $T(3/1)$ versus γ respectively, one thus obtains a series of parameters that allows an easy comparison of test samples, and therefore of the effects of preparation conditions, if any. Table III gives fit parameters of eq. (1) for all the samples tested. Negative G^*_f data (between brackets) have obviously no physical meaning and, on averaging all positive values, irrespective of the material and of the preparation conditions, a very low residual value is obtained (i.e., 1.38 ± 0.83 kPa). For a given composition, a careful examination of parameters G^*_0 , $1/A$ and B reveals no significant effects of mixing conditions, clearly smaller anyway than changes assigned to strain history effects as exhibited by filled materials (to be addressed in the next section).

Table IV gives fit parameters of eq. (2) for all PP/GCF samples. For a given composition, no significant effects of mixing conditions are seen on the nonlinear viscoelastic character, which is as expected clearly depending on the fiber content.

Within the temperature range considered for mixing operations (i.e., 170–190°C), no significant differences are thus seen in terms of (nonlinear) rheological properties of PP/GCF compounds. Consequently, for a given composition, RPA-FT results obtained on sam-

ples prepared under various mixing conditions can be averaged and the related standard deviation calculated, to capture significant variations due to GCF content.

Effects of GCF content. Figure 7 shows the typical variations of G^* versus strain curves when the fiber content increases. As can be seen, the linear viscoelastic region reduces as GCF level increases to eventually disappear (out of the experimental window). In contrast with the unfilled material, composites exhibit strain history effects that become larger with higher fiber level. All such effects are well captured by (averaged) fit parameters, at least the (extrapolated) “linear” modulus G^*_0 and the sensitivity parameter B .

As shown in Figure 8, increasing GC fiber content significantly increases the (extrapolated) linear modulus G^*_0 , as obtained when fitting experimental data with eq. (1). Average G^*_0 data (with their standard deviation as indicated) are plotted to include any variation due to mixing conditions. It is clear that the higher the fiber content, the larger the scatter, but the reinforcing effect of GCF is nevertheless seen without doubt. The larger strain history effect with higher fiber content is also clearly observed.

Figure 8 strongly suggests that the fiber reinforcing effect is at best of hydrodynamic nature without significant interactions between the PP matrix and GC fibers. The higher modulus from run 1 data is likely corresponding to initial contacts between fibers, easily disturbed by a mild strain. Run 2 data account therefore for the net reinforcing effect of GC fibers.

The strain sensitivity parameter B decreases with higher GCF content, with marginal differences between runs 1 and 2 (Fig. 9). As the polymer content decreases, the viscoelastic matrix has to support locally an increasing strain owing to the relatively

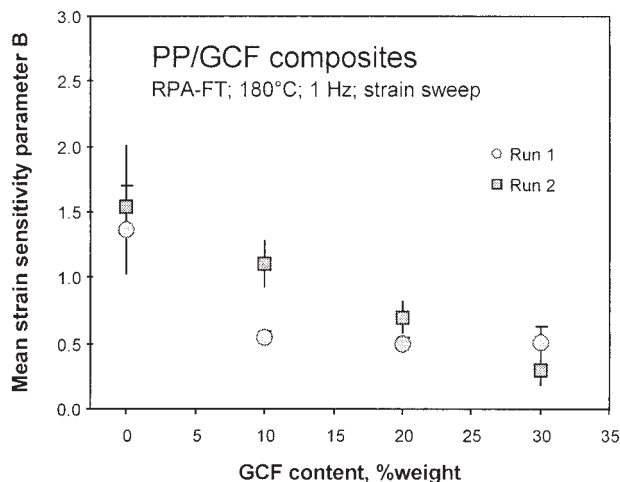


Figure 9 Effect of fibers loading on the strain sensitivity parameter of PP–GCF composites, irrespective of preparation conditions.

Mixing conditions : 190°C; 60 RPM
 RPA at 180°C ; 1 Hz; tests a &b; run 1

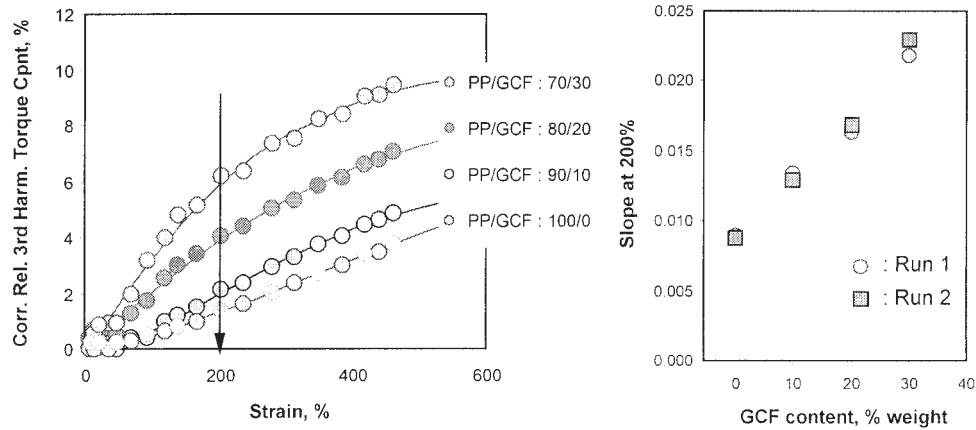


Figure 10 RPA-FT on PP/GCF composites; variation of third harmonic component with strain amplitude; effect of fiber content.

higher stiffness of GCF, but because there are no (chemical) interactions between the fibers and the polymer, the latter likely flows with respect to the former, and therefore the strain sensitivity of the bulk material is reduced.

Figure 10 compares the relative third harmonic component as recorded when submitting PP/GCF composites to strain sweep. Run 1 data are shown on the left graph and a similar figure is drawn with run 2 data. As can be seen, eq. (2) fits well with experimental

RPA at 180°C ; 1 Hz; strain sweep [Mixing conditions : 190°C; 60 RPM]

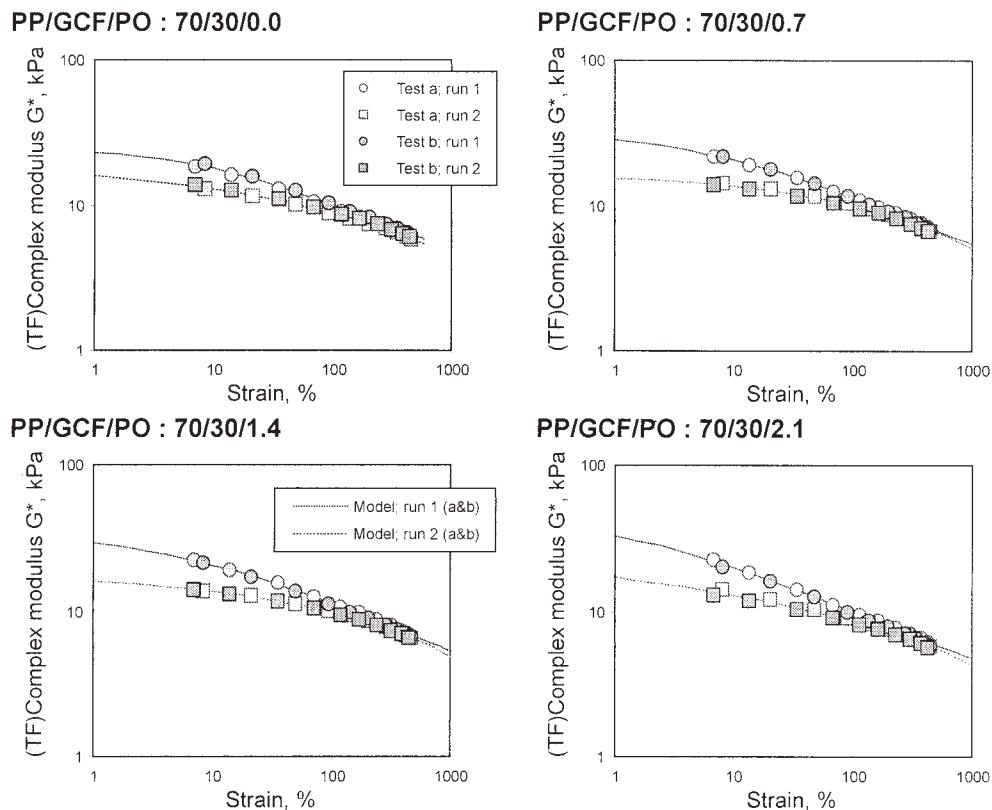


Figure 11 Complex modulus versus strain amplitude for PP/GCF/PO compounds; curves have been drawn using the corresponding fit parameters given in Table V.

TABLE V
Fit Parameters for the PP/GCF/PO Composites (RPA-FT at 180°C; 1 Hz; Strain Sweep:
Complex Modulus G^* versus Strain)

Mix temp (°C)	Rotor rate (rpm)	Runs (a and b)	G^*_0 (kPa)	G^*_f (kPa)	1/A (%)	B	r^2
<i>PP/GCF/PO = 70/30/0.7; modeling G^*_0 versus strain</i>							
190	60	1	34.18	1.74	20	0.518	0.9996
190	60	2	16.39	(-1.60)	352	0.494	0.9969
180	60	1	64.01	(-0.18)	3	0.400	0.9984
180	60	2	20.91	(-1.37)	154	0.428	0.9930
180	20	1	32.61	1.67	20	0.526	0.9994
180	20	2	14.14	0.15	316	0.626	0.9976
170	60	1	(458.90)	(-0.82)	(0)	(0.333)	0.9462
170	60	2	23.61	(-2.13)	118	0.393	0.9492
170	20	1	30.19	1.78	21	0.537	0.9982
170	20	2	15.60	(-5.10)	702	0.415	0.9985
<i>PP/GCF/PO = 70/30/1.4; modeling G^*_0 versus strain</i>							
190	60	1	37.20	1.31	14	0.485	0.9993
190	60	2	18.22	(-8.92)	1074	0.338	0.9990
180	60	1	42.40	1.25	14	0.505	0.9969
180	60	2	25.04	(-18.68)	2156	0.217	0.9991
180	20	1	35.67	0.24	12	0.429	0.9975
180	20	2	13.33	1.21	284	0.615	0.9880
170	60	1	34.53	5.08	20	0.748	0.9562
170	60	2	26.43	(-0.63)	37	0.370	0.9596
170	20	1	31.55	1.48	17	0.502	0.9997
170	20	2	13.62	(-2.35)	555	0.545	0.9992
<i>PP/GCF/PO = 70/30/2.1; modeling G^*_0 versus strain</i>							
190	60	1	53.64	1.57	3	0.460	0.9964
190	60	2	31.73	(-12.29)	68	0.180	0.9909
180	60	1	52.15	0.93	7	0.461	0.9996
180	60	2	21.35	(-2.07)	147	0.378	0.9935
180	20	1	39.47	0.45	10	0.444	0.9988
180	20	2	13.98	(-0.83)	390	0.571	0.9963
170	60	1	53.11	0.99	7	0.466	0.9989
170	60	2	28.36	(-13.44)	403	0.221	0.9986
170	20	1	33.13	1.43	14	0.493	0.9989
170	20	2	13.77	(-0.88)	382	0.546	0.9963

data and consequently calculated slopes at 200% strain provides an easy comparison feature. The progressive disappearance of any linear response at low strain is reflected by the rapid increase of torque harmonics as GCF level increases. The associated higher strain sensitivity is well quantified by the slope calculated at near midstrain range (here at 200%). The right graph shows that the higher the fiber content the larger the nonlinear character, as already seen with G^* data. Indeed the slope at 200% varies linearly with fiber level but strain history effects do not appear on $T(3/1)$ versus strain curves. Similar observations are made whatever are the preparation conditions.

Effects of compatibilizer. Typical G^* versus strain curves for GCF filled PP composites with increasing amounts of compatibilizer are shown in Figure 11. Similar figures are drawn with materials prepared under other mixing conditions. The compatibilizer does not bring any change in the nonlinear character of composites, and eq. (1) fits well the results.

Results are given in Table V in terms of fit parameters of eq. (1). Obviously wrong data are between brackets (mainly negative G^*_f values). For a given composition, no significant effects of mixing conditions are seen on parameters G^*_0 , 1/A, and B, clearly smaller anyway than changes assigned to strain history effects. Averaged values of parameters for runs 1 and 2 can therefore be used to consider any possible effect of the compatibilizer.

Figure 12 shows that when taking into account the scatter because of preparation, no significant effect of the compatibiliser can be observed on the nonlinear viscoelastic properties. Curves drawn in the figure are for visual aid only. It is worth noting that the strain history effect (i.e., difference between runs 1 and 2) is not affected at all by increasing amount of compatibilizer.

Table VI gives fit parameters of eq. (2) for all PP/GCF/PO samples. For a given composition, no significant effects of mixing conditions are seen on the non-

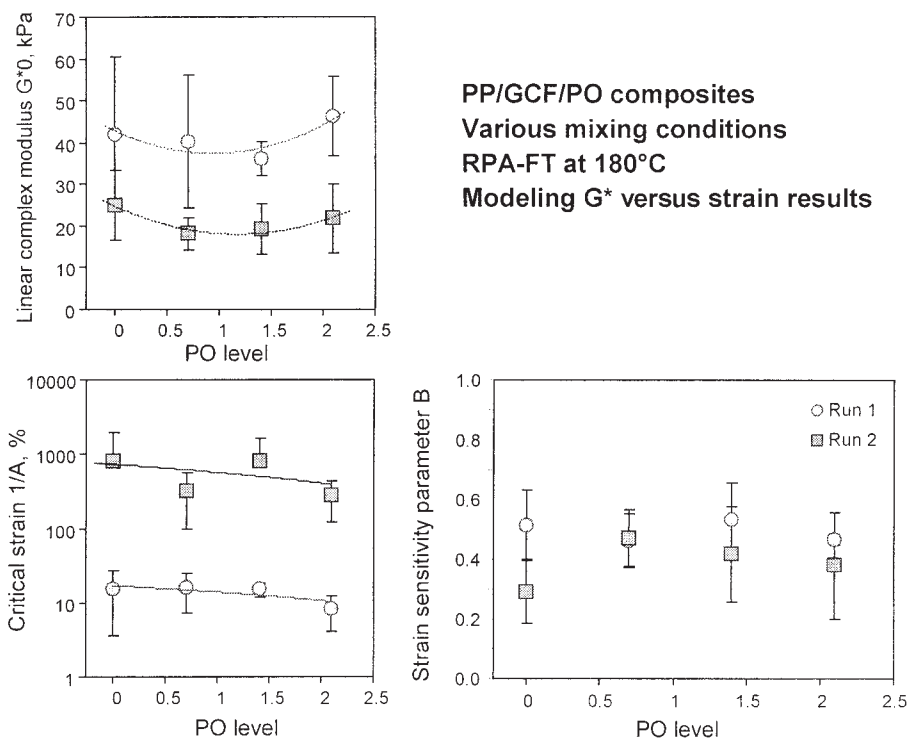


Figure 12 G^* versus strain for PP/GCF/PO composites, irrespective of preparation conditions; averaged fit parameters of eq. (1).

linear viscoelastic character, and, as illustrated by Figure 13 with slopes at 200% of the $cT(3/1)$ versus strain curves, the compatibilizer does not modify the strain sensitivity.

Mechanical data

With respect to possible applications of PP/GCF composites, essentially bending behavior is of interest in terms of mechanical properties. Flexural tests were therefore conducted at 25°C using a Universal Machine according to ASTM D790, with cross-head speed of 1 mm/min, a three-point bending system with span of 50 mm, and a cell load of 1 kN. At least 10 samples were tested for each composite. Figures 14–16 give results for PP/GCF composites obtained in different preparation conditions (mix temperature, rotor rate), with various fibers content. Comments are made in the sections hereafter.

Effect of fiber content on flexural modulus

The effect of fiber content on flexural modulus of the composites was studied by considering three levels of GCF. As can be seen, the addition of fiber produces first a decrease in flexural modulus compared to pure PP, but beyond a certain amount, additional fibers increase the property. Fibers can be considered as structural elements embedded in a polymer matrix

and, at low fiber content, the concentration of such elements is not high enough to significantly restrain the polymer molecules. Consequently, highly localized strains occur in the matrix at low stresses, causing dewetting between the polymer and the fiber and thus leaving essentially a matrix with loose, nonreinforcing fibers. As the fiber concentration increases, the stress is more evenly distributed and the composite strength and hence, the modulus increases, in agreement with explanations offered by other authors.⁷ Composites with 30% GCF exhibit flexural moduli near or superior to that of the pure PP.

Effect of mixing rate on flexural modulus

Composites were prepared in the laboratory mixer using rotor speeds 20, 40, and 60 rpm. In general, better flexural moduli are obtained when using the highest rotor speed, i.e., 60 rpm, especially at high fiber content. Such a behavior indicates that when high rotation rates are used, a better dispersion is achieved with likely a better wetting of the fiber by the molten polymer and consequently higher modulus is obtained. However, this trend is not observed with all compositions probably due to nonhomogeneity of fibers and also to the presence of powder material, which lead to a more fragile material.

TABLE VI
Fit Parameters for the PP/GCF/PO Composites (RPA-FT at 180°C; 1 Hz; Strain Sweep;
Relative Third Harmonic Component $cT(3/1)$ versus Strain)

Mix temp (°C)	Rotor rate (rpm)	Runs (a and b)	$T(3/1)_{max}$ (%)	C	D	Slope (200%)	r^2
<i>PP/GCF/PO = 70/30/0.7; modeling $cT(3/1)$ versus strain</i>							
190	60	1	9.93	0.00714	1.939	0.0255	0.9971
190	60	2	10.20	0.00678	2.535	0.0286	0.9990
180	60	1	11.55	0.00712	1.432	0.0252	0.9946
180	60	2	11.31	0.00737	2.244	0.0310	0.9971
180	20	1	10.31	0.00655	1.720	0.0065	0.9972
180	20	2	10.60	0.00608	2.187	0.0061	0.9990
170	60	1	11.90	0.00577	0.964	0.0212	0.9775
170	60	2	10.87	0.00889	2.481	0.0308	0.9941
170	20	1	10.62	0.00605	1.645	0.0251	0.9981
170	20	2	10.62	0.00608	2.110	0.0273	0.9984
<i>PP/GCF/PO = 70/30/1.4; modeling $cT(3/1)$ versus strain</i>							
190	60	1	11.45	0.00419	1.173	0.0221	0.9930
190	60	2	10.66	0.00584	2.100	0.0270	0.9957
180	60	1	11.15	0.00738	1.548	0.0253	0.9977
180	60	2	10.73	0.00767	2.327	0.0299	0.9987
180	20	1	10.44	0.00569	1.649	0.0057	0.9967
180	20	2	11.40	0.00521	2.017	0.0052	0.9967
170	60	1	11.63	0.00567	0.976	0.0209	0.9880
170	60	2	10.50	0.00875	2.310	0.0287	0.9898
170	20	1	10.07	0.00653	1.851	0.0252	0.9976
170	20	2	10.25	0.00637	2.408	0.0277	0.9988
<i>PP/GCF/PO = 70/30/2.1; modeling $cT(3/1)$ versus strain</i>							
190	60	1	9.55	0.00689	2.188	0.0257	0.9934
190	60	2	10.11	0.00606	2.563	0.0269	0.9965
180	60	1	11.16	0.00782	1.544	0.0248	0.9975
180	60	2	10.66	0.00879	2.652	0.0313	0.9987
180	20	1	10.70	0.00611	1.534	0.0061	0.9972
180	20	2	10.38	0.00676	2.380	0.0068	0.9991
170	60	1	11.44	0.00721	1.341	0.0239	0.9969
170	60	2	11.09	0.00796	2.314	0.0308	0.9980
170	20	1	9.81	0.00746	1.935	0.0251	0.9967
170	20	2	10.15	0.00656	2.300	0.0274	0.9984

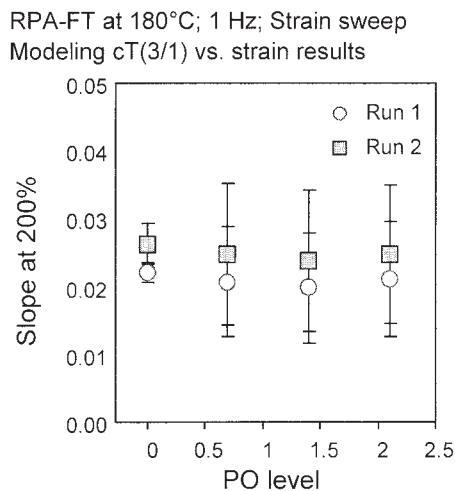


Figure 13 RPA-FT on PP/GCF/PO composites; (averaged) slopes of $T(3/1)$ versus strain curves.

Effect of mixing temperature on flexural modulus

It is well known from literature that temperature is an extremely important factor when establishing the ideal processing conditions. In this work, mix temper-

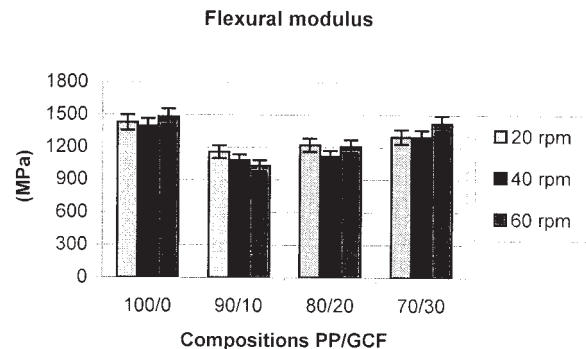


Figure 14 Flexural modulus of PP/GCF composites, prepared at 170°C, with various rotor speeds.

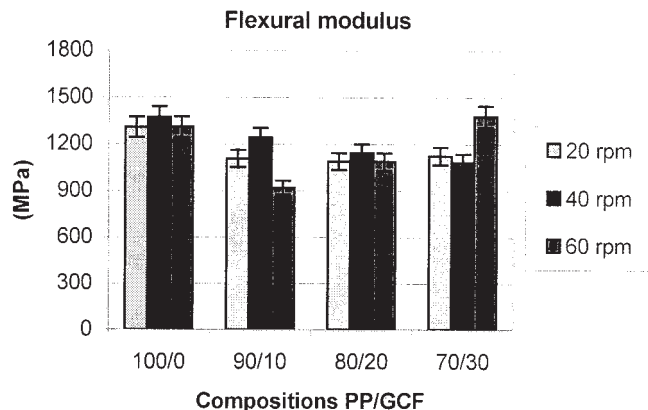


Figure 15 Flexural modulus of PP/GCF composites, prepared at 180°C, with various rotor speeds.

atures of 170, 180, and 190°C were investigated in preparing the composites. In terms of flexural modulus, no significant effect of the mixing temperature was observed in the range used.

Effect of compatibilizing agent on flexural modulus

Polyolefins are not expected to develop easy interactions, either physical (i.e., wetting) or chemical (i.e., coupling) with hydrophilic materials such as natural fibers. Consequently the use of so-called “compatibilizing agents” is generally recommended in developing polyolefins–natural fibers composites. To evaluate potential benefits of such an approach, maleated polypropylene (PO) was used in concentrations of 1, 2, and 3% with respect to PP level. Concerning flexural modulus results, the effect of PO was investigated by keeping a constant fiber content of 30%.

Figures 17–19 report the effect of increasing amount of compatibilizing agent on the flexural modulus of 70/30 PP/GCF composites prepared at various mix temperatures (170, 180, and 190°C). The flexural modulus of pure PP is also shown for comparison purposes.

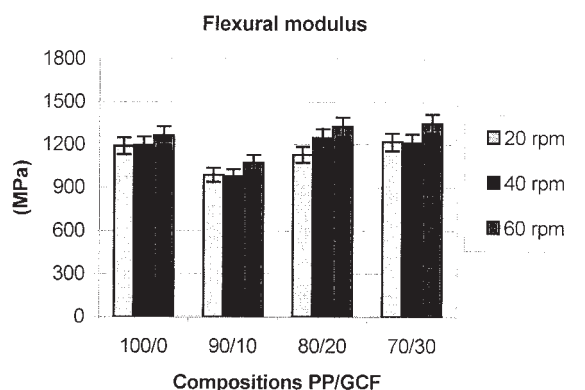


Figure 16 Flexural modulus of PP/GCF composites, prepared at 190°C, with various rotor speeds.

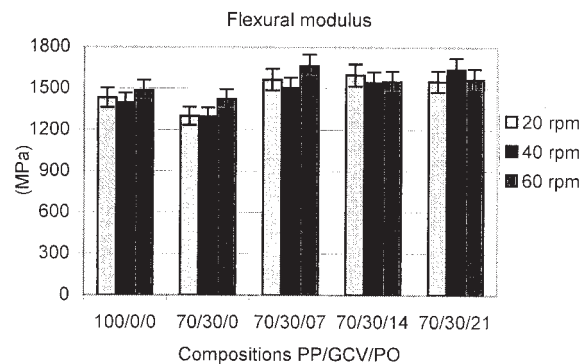


Figure 17 Flexural modulus of 70/30 PP/GCF composites with increasing level of compatibilizing agent, prepared by mixing at 170°C.

Results presented in Figures 17–19 support our previous comment that composite preparation is best achieved at 170°C, with a rotor speed of 60 rpm. Clearly, the addition of maleated polypropylene increases the flexural modulus, which is likely because of a better interfacial adhesion between fibers and matrix. Such results are in contrast with rheological data, which hardly showed a nearly negligible effect of increasing PO level. However, our flexural modulus data conform to similar effects reported in literature, where the benefit in using maleated polypropylene in cellulose fiber–PP composites was attributed to an esterification reaction believed to occur between hydroxyl groups on the cellulosic fiber and the anhydride functionality of maleated PP.⁸

For any system, one would expect an optimum concentration of compatibilizing/coupling agent. For the composites investigated in this study, it seems that the optimum level of maleated polypropylene is around 1% (of the fiber content). Compatibilizing/coupling agents are expensive additives and their use has to be considered in terms of cost/benefit balance. While the incorporation of 30% GCF to PP does not increase much the flexural modulus, the addition of 1% PO has

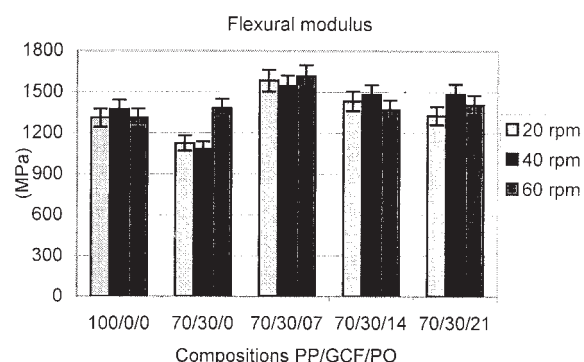


Figure 18 Flexural modulus of 70/30 PP/GCF composites with increasing level of compatibilizing agent, prepared by mixing at 180°C.

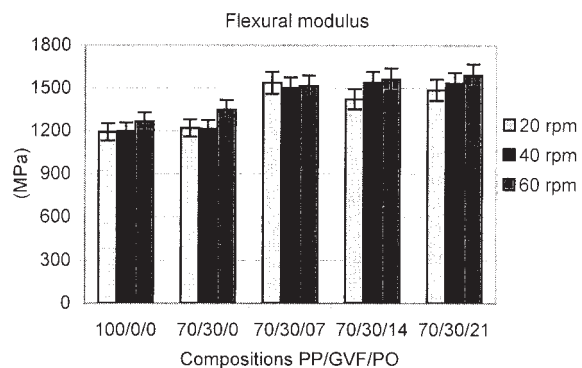


Figure 19 Flexural modulus of 70/30 PP/GCF composites with increasing level of compatibilizing agent, prepared by mixing at 190°C.

to be considered with respect to specific gains, not really appearing in the results reported here.

Morphology of PP-GCF composites as observed by SEM

Samples of PP/GCF composites, either without or with maleated polypropylene, were immersed in liquid nitrogen for a few minutes and then manually fractured. The objectives of this part of the study were to get information regarding fiber dispersion and bonding quality between fiber and matrix and to detect the presence of microdefects. Fractured surfaces were coated with a thin layer of gold and samples were observed with a JEOL JSM 5300 SEM using an acceleration voltage of 10 kV.

Figure 20 shows SEM photomicrographs of PP/GCF samples with different fiber contents prepared at mix temperature of 170°C, with various rotor speeds. From compositions (A–H), a well-defined interface between the fiber and the polymer matrix can be clearly observed. The fibers stick out of the fractured surface (as indicated by the arrows), which suggests poor adhesion. This observation is well in line with the mere thermodynamic effect of increasing fiber content as noted in the rheological part of the project and might explain the decrease in flexural modulus of compositions with fibers, when compared to the pure PP. As the rotation speed increases during the mixing process, there is however an increase of the matrix-fiber wetting which is probably due to defibrillation, which eventually gives a greater specific area on the fibers thus, favoring (physical) interactions between fibers and matrix. However there must be a limit in mixer rotor speed above which excessive fibers breakage would occur.

The effect of the coupling agent can be seen in the photomicrographs of Figure 21 (I–N). The fibers are no longer sticking out of the matrix, indicating improved interfacial adhesion, which somewhat reflects in flex-

ural modulus results. Nevertheless, varying the coupling agent content does not bring significant differences that could be detected in the samples morphology, in agreement with flexural modulus data. It seems thus that the optimal benefit of maleated polypropylene is obtained at around 1% (of the PP content).

CONCLUSIONS

Composites made of PP and GCF were thoroughly investigated with a number of complementary techniques. Dry blending of components followed by melt mixing in a laboratory mixer was demonstrated ade-

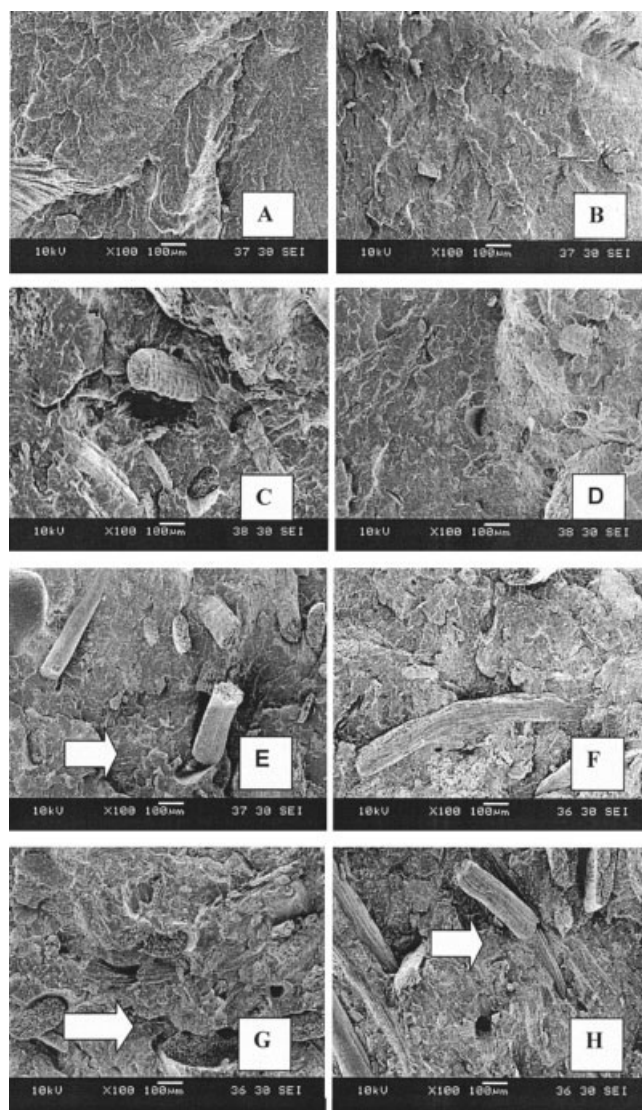


Figure 20 SEM photomicrographs of fractured surface of PP/GCF composites prepared at 170°C ($\times 100$). (A) 100/0–20 rpm; (B) 100/0–60 rpm; (C) 90/10–20 rpm; (D) 90/10–60 rpm; (E) 80/20–20 rpm; (F) 80/20–60 rpm; (G) 70/30–20 rpm; (H) 70/30–60 rpm.

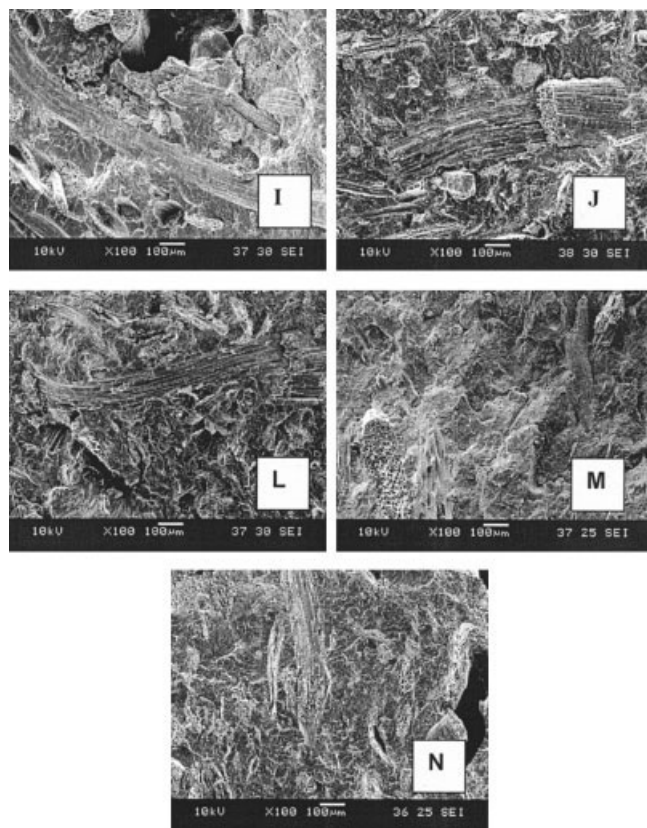


Figure 21 SEM photomicrographs of fractured surface of PP/GCF/PO composites obtained at 170°C ($\times 100$). (I) 70/30/0,7–20 rpm; (J) 70/30/0,7–60 rpm; (L) 70/30/1,4–20 rpm; (M) 70/30/1,4–60 rpm; (N) 70/30/2,1–20 rpm.

quate and fast techniques to prepare good quality PP/GCF composites.

Rheological properties of molten composites were documented using an advanced nonlinear harmonic testing technique that requires a Fourier transform treatment of the applied strain and the resulting (transmitted) stress. Results expressed in terms either of complex modulus or of relative harmonic components offers quite a complex view of the nonlinear viscoelastic response of materials but adequate modeling allows results to be summarized by a small number of parameters that can receive a precise physical meaning. Incorporating GCF into PP results in heterogeneous materials that exhibit essentially a nonlinear viscoelastic character, in contrast with the pure

PP, which has a linear viscoelastic region up to 50–60% strain. In the molten state, complex modulus increases with GCF content but in such a manner that the observed reinforcement is at best of hydrodynamic origin, without any specific chemical interaction occurring between the polymer matrix and the fibers. The addition of maleated polypropylene seems to improve the wetting of fibers by the molten polymer but the effect is so small that specific chemical reactions could hardly be considered as occurring.

Flexural modulus data show, however, an improvement when some maleated polypropylene is used in the formulation. Better wetting between the polymer matrix and the GC fibers thus result from the use of such a compatibilizing agent, as clearly demonstrated by SEM microphotographs. Whether chemical interaction occurs between PP and GCF because of the presence of maleated polypropylene remains, however, an open question since, above an optimum level of around 1% (or the PP content), higher levels of compatibilizing agent do not bring further improvement in properties. When taking all results into consideration, it is concluded that best performance PP based composites would be obtained when preparing in an internal mixer (at 170°C and 60 rpm rotor speed), formulations with 30% of GCF and 1% maleated polypropylene as compatibilizing agent.

The authors express their thanks to ExxonMobil Chemical, USA and Projeto Coco Verde S. A., Brazil, for supplying the materials used in this work.

References

1. For instance the American Physical Society through its 2002 "Statement on ethical conduct and authorship." See also Shamo, A. E.; Resnik, D. B. *Responsible Conduct of Research*; Oxford University Press: New York, 2003.
2. Leblanc, J. L.; de la Chapelle, C. *Rubber Chem Technol* 2003, 76, 287.
3. Leblanc, J. L. *J Appl Polymer Sci* 2003, 89, 1101.
4. Leblanc, J. L. *Rubber Chem Technol* 2005, 78, 54.
5. Follain, N.; Leblanc, J. L.; Furtado, C. R. G.; Visconte, L. Y. *IUPAC World Polymer Congress, Macro 2004*, Paris, July 4–9, 2004; paper P4.3–6.9.
6. Leblanc, J. L. *Ann Trans Nordic Rheol Soc* 2005, 13, 3.
7. Singleton, A. C. N.; Brillie, C. A.; Peaumont, P. W. R.; Peijs, T. *Compos B* 2003, 34, 519.
8. Joseph, P. V.; Mathew, G.; Joseph, K.; Groeninckx, G.; Thomas, S. *Compos A* 2003, 34, 275.